Circulating Fibrocytes Prepare the Lung for Cancer Metastasis by Recruiting Ly-6C+ Monocytes Via CCL2

Hendrik W. van Deventer[*], **Daniela A. Palmieri**[†], **Qing Ping Wu**[‡], **Everett C. McCook**[‡], and **Jonathan S. Serody**[*,‡,§]

[*]Department of Medicine, University of North Carolina–Chapel Hill, Chapel Hill, NC 27599

[†]Laboratory of Clinical and Experimental Vascular Biology, Institute for Hospitalization and Scientific Care University Hospital San Martino, 16132 Genoa, Italy

[‡]Lineberger Comprehensive Cancer Center, University of North Carolina–Chapel Hill, Chapel Hill, NC 27599

[§]Department of Microbiology and Immunology, University of North Carolina–Chapel Hill, Chapel Hill, NC 27599

Abstract

Fibrocytes are circulating, hematopoietic cells that express CD45 and Col1a1. They contribute to wound healing and several fibrosing disorders by mechanisms that are poorly understood. In this report, we demonstrate that fibrocytes predispose the lung to B16-F10 metastasis by recruiting Ly-6C+ monocytes. To do so, we isolated fibrocytes expressing CD45, CD11b, CD13, and Col1a1 from the lungs of wild type (WT) and $Ccr5^{-/-}$ mice. WT but not $Ccr5^{-/-}$ fibrocytes increased the number of metastatic foci when injected into $Ccr5^{-/-}$ mice (73 ± 2 versus 32 ± 5; $p < 0.001$). This process was MMP9 dependent. Injection of WT enhanced GFP+ fibrocytes also increased the number of Gr-1^{Int}, CD11b+, and enhanced GFP− monocytes. Like premetastatic-niche monocytes, these recruited cells expressed Ly-6C, CD117, and CD45. The transfer of these cells into $Ccr5^{-/-}$ mice enhanced metastasis (90 ± 8 foci) compared with B cells (27 ± 2), immature dendritic cells (31 ± 6), or alveolar macrophages (28 ± 3; $p < 0.05$). WT and $Ccl2^{-/-}$ fibrocytes also stimulated $Ccl2$ expression in the lung by 2.07 ± 0.05- and 2.78 ± 0.36-fold compared with $Ccr5^{-/-}$ fibrocytes (1.0 ± 0.06; $p < 0.05$). Furthermore, WT fibrocytes did not increase Ly-6C+ monocytes in $Ccr2^{-/-}$ mice and did not promote metastasis in either $Ccr2^{-/-}$ or $Ccl2^{-/-}$ mice. These data support our hypothesis that fibrocytes contribute to premetastatic conditioning by recruiting Ly-6C+ monocytes in a chemokine-dependent process. This work links metastatic risk to conditions that mobilize fibrocytes, such as inflammation and wound repair.

Since their discovery in 1994, fibrocytes have been described as circulating, COL1A1-expressing, hematopoietic cells (1). Derived from CD14 monocytes (2), these cells constitute <1% of the adult leukocyte pool. In health, fibrocytes are thought to promote wound healing by migrating into areas of injury and differentiating into activated fibroblasts (3). This mechanism has also been inferred from observations of several fibrosing disorders, including keloid formation (4), posttransplant bronchiolitis obliterans (5, 6), peritoneal

Address correspondence and reprint requests to Dr. Hendrik W. van Deventer, 170 Manning Drive, Campus Box 7305, Chapel Hill, NC 27599-7305. hvand@med.unc.edu.

The online version of this article contains supplemental material.

Disclosures
The authors have no financial conflicts of interest.

fibrosis, and thyroid ophthalmopathy (7). However, there is little data to substantiate this model in vivo.

A role for fibrocytes in tumor promotion has been more difficult to discern. A small number of studies have focused on the ability of fibrocytes to propagate tumor stroma. This stroma is populated with activated fibroblasts, which are characterized by their expression of α smooth muscle actin. This gene is also expressed by fibrocytes in response to TGF-β and other cytokines that promote tumor stromagenesis (8). Thus, fibrocytes can promote tumorigenesis by becoming incorporated into the stroma.

Despite the appeal of this hypothesis, this model is flawed. The small number of circulating fibrocytes likely limits their contribution to the tumor stroma. This observation has already been demonstrated in liver and dermatologic diseases associated with fibrocytes (9). Moreover, the tumor stroma has many other sources of activated fibroblasts (10). This hypothesis also fails to consider other biologic functions connected to fibrocytes. For example, fibrocytes contribute to innate immunity by the expression of antimicrobial factors (11) and adaptive immunity by Ag presentation (12). In short, fibrocytes have numerous functions that might be critical for tumor promotion. Furthermore, these functions may be independent of their ability to be incorporated into the tumor stroma.

This report establishes a new biologic role for fibrocytes as regulators of cell migration. In the process, we also provide experimental evidence that directly links fibrocytes to cancer progression. In our model, circulating fibrocytes prompt an influx of Ly-6C$^+$, Ly-6G^{lo} monocytes into the lung. This influx conditions the lung to make it more vulnerable to the invasion of cancer cells. Our model is consistent with the observations of Kaplan and others who have described the establishment of the premetastatic niche by Ly-6C$^+$ monocytes (13). We also show that this process is dependent on CCR2 and CCR5, adding to the preclinical data that establish these chemokine receptors as potential therapeutic targets.

Materials and Methods

Mice and cell lines

C57BL/6J *Ccr5*$^{-/-}$ have been previously described (14); matrix metal-loproteinase 9 knockout mice (*Mmp9*$^{-/-}$) were a gift from Dr. Lynn Matrisian. All other mouse strains were purchased from The Jackson Laboratory (Bar Harbor, ME). All animals were housed in pathogen-free conditions. *Ccr5*$^{-/-}$ × *Mmp9*$^{-/-}$ mice were produced by crossing F1 progeny of *Ccr5*$^{-/-}$ and *Mmp9*$^{-/-}$ mice.

All experiments were conducted using protocols approved by the Institutional Animal Care and Use Committee of the University of North Carolina–Chapel Hill. B16-F10, CT26, and Line 1 cell lines were purchased form American Type Culture Collection (Rockland, MD). Cell lines were verified using short tandem repeat analysis.

In vivo experiments

Pulmonary mesenchymal cells (PMCs) were isolated as described previously (15). Fibrocytes were separated from PMCs using CD45 Miltenyi beads (Bergisch Gladbach, Germany) according to the manufacturer's instructions. Immature dendritic cells were cultured from bone marrow using GM-CSF (Invitrogen) and B cells were isolated from splenocytes also using B220 beads.

Details for the melanoma metastasis model have been described previously (16). In brief, 1 × 10^5 fibrocytes in 200 μl PBS were injected via the tail vein. Twenty-four hours later, 7.5 × 10^5 B16-F10 melanoma cells were injected. Mice were euthanized 14 d later, and metastases

were counted after insufflation with Fekete's destaining solution. Experiments using other cell lines were performed in a similar manner. CT26 cells (1×10^5) were injected into C57BL/6J mice and 2×10^5 Line 1 cells were injected into BALB/c mice. Visualization of tumor nodules was enhanced by insufflation with 15% solution of India ink–PBS followed by storage in Fekete's solution.

Ex vivo experiments

The formation of enhanced GFP (EGFP) bone marrow chimeric mice has already been described (17). In brief, wild type (WT) mice were irradiated with 950 rad and injected with 3×10^6 bone marrow cells from EGFP transgenic mice. Recipient mice were maintained for 8 wk prior to their use in these studies. Details for flow cytometry and PCR have been described previously (18). Real-time PCR was performed on cDNA synthesized with M-MLV reverse transcriptase (Invitrogen) and random hexamers. Transcript number was measured with SYBR green and an ABI PRISM 7900 real-time RT-PCR system (Applied Biosystems, Foster City, CA). The copy number was normalized against the absolute mRNA amount as measured by Qubit Quantitation Platform (Invitrogen). Abs and primer sequences are given in Supplemental Table I.

Western blotting was performed on FACS-sorted pulmonary cells as previously described (18). The samples were run on a 10% SDS gel before being transferred to nitrocellulose. Primary Abs were diluted to 1:1000, and secondary Abs were diluted to 1:10,000.

Cytospin slides were prepared from a single-cell suspension of CD11b$^+$ pulmonary cells isolated by immunomagnetic beads and resuspended in 0.5% BSA. After Wright–Giemsa staining, differential counts were performed on 500 or more cells by an investigator (H.W.v.D.) blinded to the treatment.

Statistics

Unless otherwise stated, data are presented as the mean of measurements taken from three or more separate experiments. Statistical error for these means is presented as ± 1 SEM. Confidence intervals were determined using a 60% trimmed mean. The *p* values were determined by Mann–Whitney *U* test and values less than 0.05 were considered significant. The Bonferroni correction was applied to experiments involving multiple comparisons.

Results

WT fibrocytes increase metastasis in Ccr5$^{-/-}$ mice

PMCs can be isolated by culturing a single-cell suspension from the lung and harvesting the adherent cells in two to three weeks. The resultant cells increase metastasis in *Ccr5*$^{-/-}$ mice when injected prior to the injection B16-F10 melanoma cells (17). This observation is not limited to the B16-F10 cell line. As demonstrated in Fig. 1A, PMCs also increased metastasis in WT mice when transferred prior to the i.v. injection of CT26 cells (12.4 ± 1.9 versus 96.8 ± 6.4; *p* < 0.001) or Line 1 cells (1.3 ± 0.4 versus 7.9 ± 2.1; *p* < 0.001).

PMCs can be separated by CD45 expression into CD45$^-$ fibroblasts and CD45$^+$ fibrocytes. We used this distinction to isolate fibrocytes with immunomagnetic beads (Fig. 1B). The isolated cells expressed CD11b, CD13, and collagen, type 1, α 1 (Col1A1), consistent with a fibrocyte phenotype (Fig. 1C). The purity of this isolate was 91% ± 3.0% based on Col1A1 expression. The hematopoietic lineage of these fibrocytes was then confirmed by creating chimeric mice with EGFP transgenic bone marrow (Fig. 1C); 90.1 ± 0.2% of the CD45$^+$ fibrocytes isolated from the chimeric mice expressed EGFP, indicating that these cells were derived from bone marrow precursors.

To determine whether fibrocytes were the subset of PMCs that mediated pulmonary metastases, we transferred 1×10^5 fibrocytes into $Ccr5^{-/-}$ mice prior to the injection of the B16-F10 cells. These mice developed an equivalent number of metastases (73 ± 2) as WT mice injected with WT fibrocytes (85 ± 5) and WT mice that were not treated with fibrocytes (69 ± 4; Fig. 2A). The size and distribution of the metastatic colonies were similar with all three treatments; the only difference was the number of metastases (Supplemental Fig. 1). All three of these groups had significantly more pulmonary metastases than uninjected $Ccr5^{-/-}$ mice (49 ± 3; $p < 0.01$) or mice injected with $Ccr5^{-/-}$ fibrocytes (32 ± 5; $p < 0.001$). CD45$^-$ fibroblasts, however, did not increase metastasis compared with fibrocytes (72 ± 10 versus 113 ± 4; $p < 0.002$; Fig. 2B). Therefore, these data indicate that the fraction of PMCs promoting lung metastases is the CD45$^+$ fibrocyte fraction.

WT fibrocytes promote metastasis via MMP9

WT PMCs increase metastasis by inducing MMP9 (16). To determine whether fibrocytes promote metastasis by an MMP9-dependent mechanism, we transferred WT fibrocytes into $Mmp9^{-/-}$ mice. As hypothesized, pulmonary metastases were not increased in $Mmp9^{-/-}$ mice as they were in $Ccr5^{-/-}$ mice (43 ± 2 versus 96 ± 6; $p < 0.01$; Fig. 2C, Supplemental Fig. 1).

These data suggest that CCR5 and MMP9 are part of the same prometastatic pathway. We looked for the potential additive benefit of inhibiting both CCR5 and MMP9 by crossing $Mmp9^{-/-}$ mice with $Ccr5^{-/-}$ mice. As shown in Fig. 2D, metastasis in the double knockout was not inhibited more than either $Ccr5^{-/-}$ or $Mmp9^{-/-}$ mice (48 ± 2 versus 51 ± 3 versus 37 ± 3; $p = $ NS). All three of these groups had fewer metastases than did the control WT mice (72 ± 6; $p < 0.05$). Therefore, our data indicated that fibrocytes were critical to the promotion of pulmonary metastases and that this process required MMP9 and CCR5, which function via a *cis*-mediated mechanism.

WT fibrocytes recruit Ly-6C$^+$, Ly-6G^{low} monocytic cells

Next, we sought the mechanism by which fibrocytes increase pulmonary metastases. Previous work suggested that WT PMCs induced the migration of CD11b$^+$ cells into the lung. We reexamined this finding by injecting EGFP$^+$ fibrocytes from WT and $Ccr5^{-/-}$ mice into $Ccr5^{-/-}$ animals. This design allowed us to exclude the injected fibrocytes by gating on the EGFP$^-$ cells. As before, WT EGFP$^+$ fibrocytes induced a statistically significant increase in CD11b$^+$ cells in the lung ($p < 0.02$; Fig. 3A). No such increase was found in CD11b$^-$ cells after the injection of fibrocytes. Injection of $Ccr5^{-/-}$ fibrocytes failed to increase CD11b$^+$ or CD11b$^-$ cells.

Flow cytometry was then used to identify the following CD11b$^+$ cells: monocytes, macrophages, dendritic cells, granulocytic (Gr-1^{Hi}) myeloid derived suppressor cells (MDSCs), and monocytic (Gr-1^{Int}) MDSCs (Fig. 3B). All other CD11b$^+$ cells were labeled as myeloid cells, not otherwise specified (NOS). Using this approach, the monocytic MDSC was the only population significantly increased by WT but not $Ccr5^{-/-}$ fibrocytes ($p < 0.02$; Fig. 3C).

Because Gr-1 is a nonspecific marker for myeloid cells, the Gr-1^{Int} population was analyzed further with Ly-6C and Ly-6G Abs. As shown in Fig. 3D, WT fibrocytes did not increase the percentage of Ly-6G$^+$ cells (13.6 ± 1.1 versus $13.3 \pm 2.5\%$; $p = $ NS). However, Ly-6C$^+$, Ly-6G^{low} cells were significantly increased (17.0 ± 2.0 versus $11.7 \pm 2.2\%$; $p < 0.01$) after the injection of WT fibrocytes. These flow cytometry results were corroborated by performing differential counts on cytospin preparations of the CD11b$^+$ cells. Monocytes were more prevalent in mice injected with WT fibrocytes compared with the controls (33.2

± 1.3% versus 25.2 ± 3.0% versus 19.6 ± 1.1%; $p < 0.05$; Fig. 3E). From these data, we concluded that WT fibrocytes enhanced the recruitment of Ly-6C$^+$, Ly-6G^{low} monocytes into the lung.

Ly-6C$^+$, Ly-6G^{low} monocytic cells are consistent with premetastatic monocytes

The premetastatic niche is formed by monocytes characterized by the expression of CD11b, Ly-6C, CD45, CD117, and Itga4 (19). As demonstrated above, fibrocytes recruited monocytes that expressed CD11b and Ly-6C. These monocytes also expressed CD45, CD117, but not CD11c (Fig. 4A). The presence of Itga4 but not Mmp9 was shown by Western blotting applied to monocytes isolated from the lungs of fibrocyte-injected mice (Fig. 4B).

The defining property of premetastatic monocytes is their capacity to promote metastasis. This ability was tested by isolating Ly-6C$^+$ cells from $Ccr5^{-/-}$ mice injected with WT fibrocytes and then transferring 2×10^5 of these cells into mice that had not received fibrocytes (Fig. 4C). As shown in Fig. 4D, fibrocyte-recruited Ly-6C$^+$ monocytes significantly increased metastasis in $Ccr5^{-/-}$ mice whereas B cells and immature dendritic cells did not (90 ± 8 versus 26 ± 2 and 31 ± 6 respectively; $p < 0.01$).

The importance of Ly-6C$^+$ monocytes in this model was further strengthened by depleting the Ly-6G^{++} cells. These cells could be depleted from the lung with the Ly-6G Ab or with the Gr-1 Ab (18) (Fig. 4E, 4F). Depletion of these cells with either Ab had no effect on the fibrocytes' ability to increase metastasis (Fig. 4G). Therefore, the promotion of metastasis by fibrocytes was not dependent on the recruitment of Ly-6G^{++} cells. Instead, the prometastatic effect of fibrocytes was limited to their influence on the population of Ly-6C$^+$ myeloid cells.

Ly-6C$^+$ cells are recruited by CCL2-CCR2 axis

Next, we evaluated the fibrocytes' dependence on Ly-6C$^+$ cells in the promotion of lung metastasis. Ab depletion of the Ly-6C$^+$ cells is not possible because of the ubiquitous expression of this protein. However, the migration of Ly-6C$^+$ monocytes can be inhibited by blocking CCR2. In the $Ccr2^{-/-}$ mouse, injection of WT fibrocytes did not increase the number of Ly-6C$^+$ cells in the lung (5.8 ± 0.6 × 10^5 versus 7.1 ± 2.4 × 10^5 cells; $p =$ NS; Fig. 5A). The only significant increase in cell number came after the injection of WT fibrocytes into $Ccr5^{-/-}$ mice (17.3 ± 0.2 × 10^5 cells; $p < 0.05$). The percentage of monocytes was also not increased in the $Ccr2^{-/-}$ mice as measured by differential counts of CD11b$^+$ cells recognized on cytospin slides (22.7 ± 0.7% versus 22.7 ± 2.2%; Fig. 5B).

If the recruitment of Ly-6C$^+$ myeloid cells was critical to the ability of fibrocytes to enhance metastasis, then fibrocytes should not increase metastasis in the $Ccr2^{-/-}$ mouse. As expected, WT, $Ccr2^{-/-}$, or $Ccr5^{-/-}$ fibrocytes did not increase in metastasis in $Ccr2^{-/-}$ mice (Fig. 5C). Once again, the size and distribution of the metastatic colonies was substantially different (Supplemental Fig. 2). These results confirmed the requisite role of the migration of CCR2-expressing Ly-6C$^+$ cells in this process.

The predominant ligand for CCR2 is CCL2. In our model, CCL2 could be generated by migrating fibrocytes or by the surrounding pulmonary stroma. To answer this question, $Ccl2$ was measured in the lung of $Ccr5^{-/-}$ mice before and after injection with WT and $Ccl2^{-/-}$ fibrocytes. Using real-time PCR, WT and $Ccl2^{-/-}$ fibrocytes increased $Ccl2$ expression by 2.07 ± 0.05-fold and 2.78 ± 0.36-fold, respectively ($p =$ NS). Both were significantly greater than baseline expression of $Ccl2$ (1.0 ± 0.06; $p < 0.05$). These results suggested that $Ccl2$ induction by fibrocytes was not cell intrinsic because fibrocytes lacking $Ccl2$ induced similar levels of the chemokine in the lung.

The importance of fibrocyte-generated CCL2 on metastasis was tested by injecting $Ccr5^{-/-}$ mice with WT and $Ccl2^{-/-}$ fibrocytes. As shown in Fig. 5D, metastasis was increased in $Ccr5^{-/-}$ mice by the injection of WT and $Ccl2^{-/-}$ fibrocytes compared with control (75 ± 12, 76 ± 6, 45 ± 6; $p < 0.05$). In contrast, WT and $Ccl2^{-/-}$ fibrocytes did not increase metastasis in $Ccl2^{-/-}$ mice (52 ± 6, 53 ± 13) compared with $Ccl2^{-/-}$ mice that had not received fibrocytes (51 ± 7). All three groups had fewer metastases than did $Ccr5^{-/-}$ mice injected with WT fibrocytes (96 ± 5; p 0.02). These results indicate that the injection of fibrocytes mediates the expression of CCL2 by pulmonary cells.

Discussion

By adoptively transferring WT fibrocytes into $Ccr5^{-/-}$ mice, this report provides confirmation that fibrocytes promote lung metastasis. We intentionally injected fibrocytes before injecting tumor cells. This "premetastatic" model allowed us to study changes induced by the fibrocytes that were not influenced by local tumor. As a result, we were able to show that fibrocytes promoted metastasis by recruiting Ly-6C^{+} monocytes. Therefore, our data suggest a new function for fibrocytes as regulators of cellular migration.

Fibrocytes have been described in precancerous lesions and in the peritumoral stroma (20, 21). Tumor stroma, however, has significantly reduced numbers of fibrocytes but increased numbers of myofibroblasts. These observational studies assumed the increase in myofibroblasts was due to the transition of fibrocytes to activated fibroblasts. However, these studies were correlative and ignored the predominant sources of tumor-associated fibroblasts. Pericytes, adipocytes, and epithelial cells are all capable of trans-differentiating into stromal cells (22). Bone marrow mesenchymal cells also contribute to the myofibroblast pool (23). Given the large number of cells capable of generating stromal cells, the overall contribution of a small population of migrating fibrocytes could be considered inconsequential. Although the transition from fibrocyte to fibroblast is well documented, incorporation into the stroma might not be their primary mechanism of promoting disease. Our model would add additional complexity to the interpretations of data from these older studies by demonstrating that fibrocytes recruit immunosuppressive myeloid cells to the lung. Such a function would distinguish these cells from other fibroblast precursors.

Premetastatic niches are clusters of bone marrow–derived cells that facilitate the invasion and survival of circulating tumor cells (24). Initially described by Kaplan et al. (13) and later confirmed by several additional investigators, the cells of this niche express CD11b^{+} (25), Gr-1^{+} (26), Itga4 (13), CD133, CD34, cKit (CD117), and VLA4 (19). This description is consistent with the Ly-6C^{+} monocytes recruited by fibrocytes described in the current work. Furthermore, adoptive transfer of these cells established their functional capacity as premetastatic promoters of metastasis.

Experimental evidence for the creation of premetastatic niches is growing. Premetastatic infiltration by monocytes has been described in models of pancreatic (27) and breast cancer (28). Mechanisms underlying the creation of such niches are also beginning to emerge (29), (25), (30), (31). The predominant mechanism of monocyte recruitment in this study was the induction of CCL2. This chemokine has been associated with poorer outcomes in several cancers, including myeloma, breast cancer, and prostate cancer (30). The receptor, CCR2, promotes invasion of myeloid cells after treatment, which creates a greater risk of relapse (32). Polymorphisms that increase CCR2 expression are associated with a greater risk of death in prostate (33) and gastric cancer (34). In the murine metastasis models, Ccl2 has been implicated in the influx of Gr-1^{+} monocytes in pulmonary metastasis, but not primary mammary tumors in mice. Blockade of Ccl2 inhibits these inflammatory monocytes and prolongs survival (35).

CCL2 can also contribute to the promotion of metastasis by inducing the expression of MMP9 (36). This metalloproteinase is required for the formation of premetastatic niche (37) and for the induction of angiogenesis (38). Our model was also dependent on the expression of MMP9. Together, these signals can establish a positive feedback loop. MMP9 contributes to the recruitment of additional monocytes in a cathepsin-L–dependent manner (39), and CCL2 recruits additional fibrocytes (40). These mechanisms would explain why small numbers of fibrocytes have such profound effects on metastasis.

These data could help to clarify aspects of tumor biology that are poorly understood. For example, several studies have suggested that surgery could have prometastatic effects (41). Peak mobilization of fibrocytes occurs between 3 and 7 d after wound formation (42). These circulating fibrocytes could subsequently condition the stroma for cancer cells emigrating from stem cell niches in the bone marrow. Although this mechanism has not been studied in cancer patients, a similar phenomenon has been documented for endothelial progenitor cells (43).

Our data suggest means of interrupting this pathway, which could create a new means of preventing metastasis. Our work has focused on decreasing fibrocyte migration through the chemokine pathways. Fibrocyte migration has also been decreased by inhibition of MTOR (44), the angiotensin II type 1 receptor (45), Kcs3.1K+ channels (46) or CXCR4 (47). Inhibition of fibrocytes and monocytes might also be possible through the development of dual CCR5/CCR2 inhibitors (48).

In summary, we have presented a mechanism by which fibrocytes can prepare the pulmonary stroma for metastasis by recruiting Ly-6C$^+$, Ly-6G^{low} monocytes through the induction of CCL2. The interactions among fibrocytes, monocytes, and cancer cells depend on CCR5, CCR2, and MMP9. This work has implications for conditions that promote fibrocyte migration, such as surgery, and it provides a rationale for novel combinations of currently existing therapeutics.

Supplementary Material

Refer to Web version on PubMed Central for supplementary material.

Acknowledgments

Abbreviations used in this article

|	
EGFP	enhanced GFP
PMC	pulmonary mesenchymal cell
WT	wild type

References

1. Bucala R, Spiegel LA, Chesney J, Hogan M, Cerami A. Circulating fibrocytes define a new leukocyte subpopulation that mediates tissue repair. Mol Med. 1994; 1:71–81. [PubMed: 8790603]
2. Bucala R. Review Series – Inflammation & fibrosis fibrocytes and fibrosis. QJM. 2012; 105:505–508. [PubMed: 22627257]

3. Quan TE, Cowper S, Wu SP, Bockenstedt LK, Bucala R. Circulating fibrocytes: collagen-secreting cells of the peripheral blood. Int J Biochem Cell Biol. 2004; 36:598–606. [PubMed: 15010326]

4. Iqbal SA, Sidgwick GP, Bayat A. Identification of fibrocytes from mesenchymal stem cells in keloid tissue: a potential source of abnormal fibroblasts in keloid scarring. Arch Dermatol Res. 2012; 304:665–671. [PubMed: 22407077]

5. Todd JL, Palmer SM. Bronchiolitis obliterans syndrome: the final frontier for lung transplantation. Chest. 2011; 140:502–508. [PubMed: 21813529]

6. LaPar DJ, Burdick MD, Emaminia A, Harris DA, Strieter BA, Liu L, Robbins M, Kron IL, Strieter RM, Lau CL. Circulating fibrocytes correlate with bronchiolitis obliterans syndrome development after lung transplantation: a novel clinical biomarker. Ann Thorac Surg. 2011; 92:470–477. discussion 477. [PubMed: 21801908]

7. Gillespie EF, Papageorgiou KI, Fernando R, Raychaudhuri N, Cockerham KP, Charara LK, Goncalves ACP, Zhao SX, Ginter A, Lu Y, et al. Increased expression of TSH receptor by fibrocytes in thyroid-associated ophthalmopathy leads to chemokine production. J Clin Endocrinol Metab. 2012; 97:E740–E746. [PubMed: 22399514]

8. Hong KM, Belperio JA, Keane MP, Burdick MD, Strieter RM. Differentiation of human circulating fibrocytes as mediated by transforming growth factor-β and peroxisome proliferator-activated receptor γ. J Biol Chem. 2007; 282:22910–22920. [PubMed: 17556364]

9. Higashiyama R, Nakao S, Shibusawa Y, Ishikawa O, Moro T, Mikami K, Fukumitsu H, Ueda Y, Minakawa K, Tabata Y, et al. Differential contribution of dermal resident and bone marrow-derived cells to collagen production during wound healing and fibrogenesis in mice. J Invest Dermatol. 2011; 131:529–536. [PubMed: 20962852]

10. Kalluri R, Zeisberg M. Fibroblasts in cancer. Nat Rev Cancer. 2006; 6:392–401. [PubMed: 16572188]

11. Kisseleva T, von Köckritz-Blickwede M, Reichart D, McGillvray SM, Wingender G, Kronenberg M, Glass CK, Nizet V, Brenner DA. Fibrocyte-like cells recruited to the spleen support innate and adaptive immune responses to acute injury or infection. J Mol Med. 2011; 89:997–1013. [PubMed: 21499735]

12. Chesney J, Bacher M, Bender A, Bucala R. The peripheral blood fibrocyte is a potent antigen-presenting cell capable of priming naive T cells in situ. Proc Natl Acad Sci USA. 1997; 94:6307–6312. [PubMed: 9177213]

13. Kaplan RN, Riba RD, Zacharoulis S, Bramley AH, Vincent L, Costa C, MacDonald DD, Jin DK, Shido K, Kerns SA, et al. VEGFR1-positive haematopoietic bone marrow progenitors initiate the pre-metastatic niche. Nature. 2005; 438:820–827. [PubMed: 16341007]

14. Kuziel WA, Dawson TC, Quinones M, Garavito E, Chenaux G, Ahuja SS, Reddick RL, Maeda N. CCR5 deficiency is not protective in the early stages of atherogenesis in apoE knockout mice. Atherosclerosis. 2003; 167:25–32. [PubMed: 12618265]

15. Schüler T, Körnig S, Blankenstein T. Tumor rejection by modulation of tumor stromal fibroblasts. J Exp Med. 2003; 198:1487–1493. [PubMed: 14623905]

16. van Deventer HW, Wu QP, Bergstralh DT, Davis BK, O'Connor BP, Ting JP, Serody JS. C-C chemokine receptor 5 on pulmonary fibrocytes facilitates migration and promotes metastasis via matrix metalloproteinase 9. Am J Pathol. 2008; 173:253–264. [PubMed: 18535183]

17. van Deventer HW, O'Connor W Jr, Brickey WJ, Aris RM, Ting JP, Serody JS. C-C chemokine receptor 5 on stromal cells promotes pulmonary metastasis. Cancer Res. 2005; 65:3374–3379. [PubMed: 15833871]

18. van Deventer HW, Burgents JE, Wu QP, Woodford RM, Brickey WJ, Allen IC, McElvania-Tekippe E, Serody JS, Ting JP. The inflammasome component NLRP3 impairs antitumor vaccine by enhancing the accumulation of tumor-associated myeloid-derived suppressor cells. Cancer Res. 2010; 70:10161–10169. [PubMed: 21159638]

19. Peinado H, Lavotshkin S, Lyden D. The secreted factors responsible for pre-metastatic niche formation: old sayings and new thoughts. Semin Cancer Biol. 2011; 21:139–146. [PubMed: 21251983]

20. Barth PJ, Ramaswamy A, Moll R. CD34(+) fibrocytes in normal cervical stroma, cervical intraepithelial neoplasia III, and invasive squamous cell carcinoma of the cervix uteri. Virchows Arch. 2002; 441:564–568. [PubMed: 12461613]

21. Barth PJ, Schenck zu Schweinsberg T, Ramaswamy A, Moll R. CD34+ fibrocytes, alpha-smooth muscle antigen-positive myofibroblasts, and CD117 expression in the stroma of invasive squamous cell carcinomas of the oral cavity, pharynx, and larynx. Virchows Arch. 2004; 444:231–234. [PubMed: 14758552]

22. Xouri G, Christian S. Origin and function of tumor stroma fibroblasts. Semin Cell Dev Biol. 2010; 21:40–46. [PubMed: 19944178]

23. De Boeck A, Narine K, De Neve W, Mareel M, Bracke M, De Wever O. Resident and bone marrow-derived mesenchymal stem cells in head and neck squamous cell carcinoma. Oral Oncol. 2010; 46:336–342. [PubMed: 20219413]

24. Condeelis J, Pollard JW. Macrophages: obligate partners for tumor cell migration, invasion, and metastasis. Cell. 2006; 124:263–266. [PubMed: 16439202]

25. Hiratsuka S, Watanabe A, Aburatani H, Maru Y. Tumour-mediated upregulation of chemoattractants and recruitment of myeloid cells predetermines lung metastasis. Nat Cell Biol. 2006; 8:1369–1375. [PubMed: 17128264]

26. McGovern M, Voutev R, Maciejowski J, Corsi AK, Hubbard EJ. A "latent niche" mechanism for tumor initiation. Proc Natl Acad Sci USA. 2009; 106:11617–11622. [PubMed: 19564624]

27. Clark CE, Hingorani SR, Mick R, Combs C, Tuveson DA, Vonderheide RH. Dynamics of the immune reaction to pancreatic cancer from inception to invasion. Cancer Res. 2007; 67:9518–9527. [PubMed: 17909062]

28. Yang L, Huang J, Ren X, Gorska AE, Chytil A, Aakre M, Carbone DP, Matrisian LM, Richmond A, Lin PC, Moses HL. Abrogation of TGF beta signaling in mammary carcinomas recruits Gr-1+CD11b+ myeloid cells that promote metastasis. Cancer Cell. 2008; 13:23–35. [PubMed: 18167337]

29. Gil-Bernabé AM, Ferjanič Š, Tlalka M, Zhao L, Allen PD, Im JH, Watson K, Hill SA, Amirkhosravi A, Francis JL, et al. Recruitment of monocytes/macrophages by tissue factor-mediated coagulation is essential for metastatic cell survival and premetastatic niche establishment in mice. Blood. 2012; 119:3164–3175. [PubMed: 22327225]

30. Craig MJ, Loberg RD. CCL2 (Monocyte Chemoattractant Protein-1) in cancer bone metastases. Cancer Metastasis Rev. 2006; 25:611–619. [PubMed: 17160712]

31. Grange C, Tapparo M, Collino F, Vitillo L, Damasco C, Deregibus MC, Tetta C, Bussolati B, Camussi G. Microvesicles released from human renal cancer stem cells stimulate angiogenesis and formation of lung pre-metastatic niche. Cancer Res. 2011; 71:5346–5356. [PubMed: 21670082]

32. Nakasone ES, Askautrud HA, Kees T, Park JH, Plaks V, Ewald AJ, Fein M, Rasch MG, Tan YX, Qiu J, et al. Imaging tumor-stroma interactions during chemotherapy reveals contributions of the microenvironment to resistance. Cancer Cell. 2012; 21:488–503. [PubMed: 22516258]

33. Kucukgergin C, Isman FK, Cakmakoglu B, Sanli O, Seckin S. Association of polymorphisms in MCP-1, CCR2, and CCR5 genes with the risk and clinicopathological characteristics of prostate cancer. DNA Cell Biol. 2012; 31:1418–1424. [PubMed: 22612293]

34. Gawron AJ, Fought AJ, Lissowska J, Ye W, Zhang X, Chow WH, Beane Freeman LE, Hou L. Polymorphisms in chemokine and receptor genes and gastric cancer risk and survival in a high risk Polish population. Scand J Gastroenterol. 2011; 46:333–340. [PubMed: 21091093]

35. Qian BZ, Li J, Zhang H, Kitamura T, Zhang J, Campion LR, Kaiser EA, Snyder LA, Pollard JW. CCL2 recruits inflammatory monocytes to facilitate breast-tumour metastasis. Nature. 2011; 475:222–225. [PubMed: 21654748]

36. Richardson VJ. Divergent and synergistic regulation of matrix metalloprotease production by cytokines in combination with C-C chemokines. Int J Immunopathol Pharmacol. 2010; 23:715–726. [PubMed: 20943041]

37. Hiratsuka S, Nakamura K, Iwai S, Murakami M, Itoh T, Kijima H, Shipley JM, Senior RM, Shibuya M. MMP9 induction by vascular endothelial growth factor receptor-1 is involved in lung-specific metastasis. Cancer Cell. 2002; 2:289–300. [PubMed: 12398893]

38. Pollard JW. Tumour-educated macrophages promote tumour progression and metastasis. Nat Rev Cancer. 2004; 4:71–78. [PubMed: 14708027]

39. Sun M, Chen M, Liu Y, Fukuoka M, Zhou K, Li G, Dawood F, Gramolini A, Liu PP. Cathepsin-L contributes to cardiac repair and remodelling post-infarction. Cardiovasc Res. 2011; 89:374–383. [PubMed: 21147810]

40. Liao WT, Yu HS, Arbiser JL, Hong CH, Govindarajan B, Chai CY, Shan WJ, Lin YF, Chen GS, Lee CH. Enhanced MCP-1 release by keloid CD14+ cells augments fibroblast proliferation: role of MCP-1 and Akt pathway in keloids. Exp Dermatol. 2010; 19:e142–e150. [PubMed: 20100200]

41. Demicheli R, Retsky MW, Hrushesky WJM, Baum M. Tumor dormancy and surgery-driven interruption of dormancy in breast cancer: learning from failures. Nat Clin Pract Oncol. 2007; 4:699–710. [PubMed: 18037874]

42. Mori L, Bellini A, Stacey MA, Schmidt M, Mattoli S. Fibrocytes contribute to the myofibroblast population in wounded skin and originate from the bone marrow. Exp Cell Res. 2005; 304:81–90. [PubMed: 15707576]

43. Laing AJ, Dillon JP, Condon ET, Street JT, Wang JH, McGuinness AJ, Redmond HP. Mobilization of endothelial precursor cells: systemic vascular response to musculoskeletal trauma. J Orthop Res. 2007; 25:44–50. [PubMed: 17001704]

44. Mehrad B, Burdick MD, Strieter RM. Fibrocyte CXCR4 regulation as a therapeutic target in pulmonary fibrosis. Int J Biochem Cell Biol. 2009; 41:1708–1718. [PubMed: 19433312]

45. Sakai N, Wada T, Matsushima K, Bucala R, Iwai M, Horiuchi M, Kaneko S. The renin-angiotensin system contributes to renal fibrosis through regulation of fibrocytes. J Hypertens. 2008; 26:780–790. [PubMed: 18327089]

46. Cruse G, Singh SR, Duffy SM, Doe C, Saunders R, Brightling CE, Bradding P. Functional KCa3.1 K+ channels are required for human fibrocyte migration. J Allergy Clin Immunol. 2011; 128:1303–1309. e2. [PubMed: 21872912]

47. Song JS, Kang CM, Kang HH, Yoon HK, Kim YK, Kim KH, Moon HS, Park SH. Inhibitory effect of CXC chemokine receptor 4 antagonist AMD3100 on bleomycin induced murine pulmonary fibrosis. Exp Mol Med. 2010; 42:465–472. [PubMed: 20498529]

48. Zhao Q. Dual targeting of CCR2 and CCR5: therapeutic potential for immunologic and cardiovascular diseases. J Leukoc Biol. 2010; 88:41–55. [PubMed: 20360402]
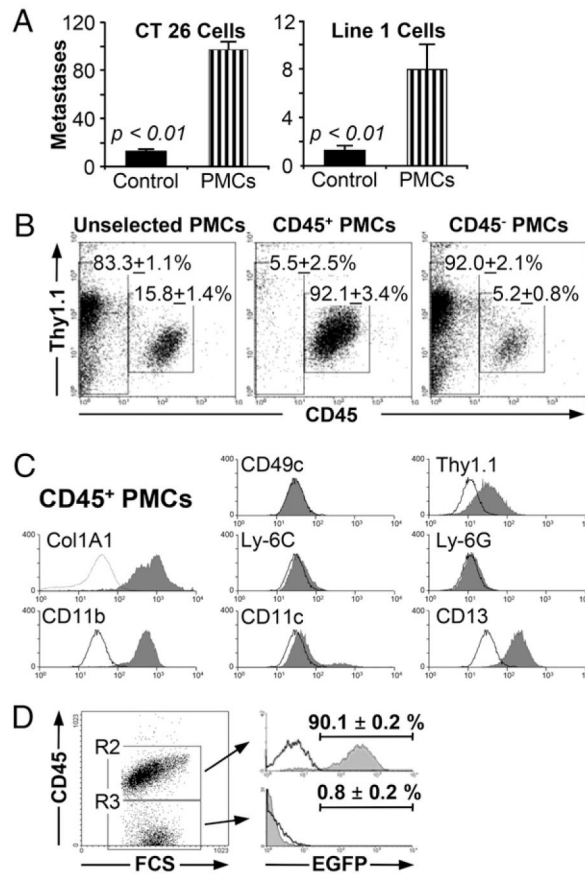
FIGURE 1.
Characterization and isolation of fibrocytes. (**A**) Injection of WT pulmonary mesenchymal cells increases metastases with CT26 and Line 1 tumor cells. The graph shows the number of metastatic foci in BALB/c mice injected with 4×10^5 pulmonary mesenchymal cells (PMCs; striped bars) compared with PBS-injected controls (solid bars). The graph on the *left* demonstrates a 7.8-fold increase in metastasis after injection with 1×10^5 CT26 cells ($n = 20$). The graph on the *right* shows a 6.2-fold increase after an injection with 2×10^5 Line 1 cells ($n = 22$). (**B**) CD45$^+$ fibrocytes can be isolated using immunomagnetic bead selection. Pulmonary mesenchymal cells were isolated from minced lung cultures as described. These cells were incubated with CD45 immunomagnetic beads and selected with Miltenyi magnetic columns. Representative dot plots are shown for cells prior to selection (*left*), CD45 selected cells (*center*), and flow through cells (*right; n = 4*). (**C**) CD45$^+$ PMCs are phenotypically consistent with fibrocytes. Flow cytometry was performed on PMCs for the indicated markers. Representative histograms are shown for CD45$^+$ cells (solid gray) and isotype control (black line). (**D**) CD45$^+$ fibrocytes originate in the bone marrow. WT bone marrow chimeric mice were formed by injecting 3×10^6 bone marrow cells from EGFP transgenic mice into irradiated WT mice. Six to eight weeks later, the lungs were harvested and PMCs were isolated using the standard 2-wk protocol. The cells were then assessed by flow cytometry. The dot plot on the left shows PMCs characterized by forward scatter and CD45 expression. The histogram on the *top right* shows the percentage of EGFP$^+$ cells taken from the CD45$^+$ PMCs (R2). The histogram on the *bottom* shows EGFP$^+$ cells taken from the CD45$^-$ PMCs (R3). The unfilled black line is EGFP expression for WT mice injected with WT (non-EGFP) marrow ($n = 8$).
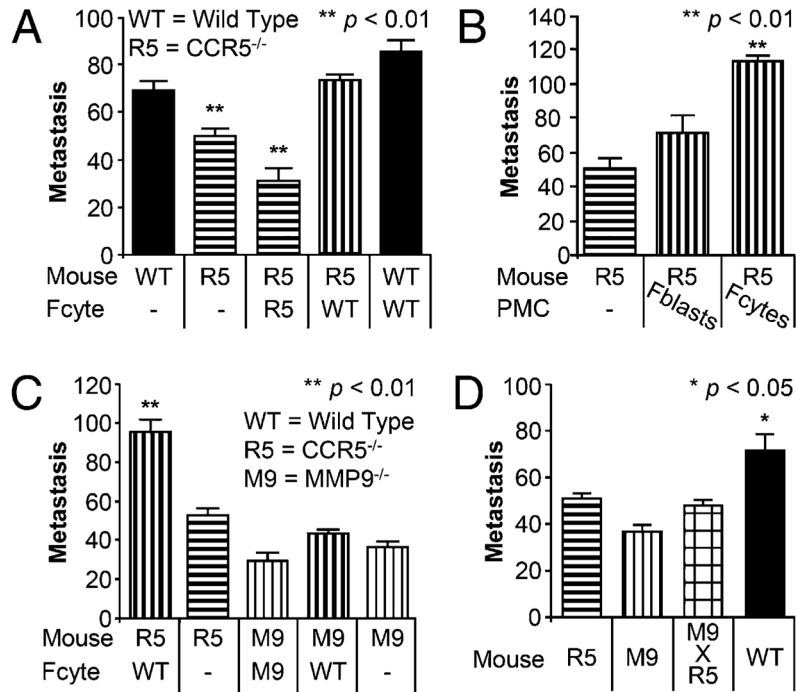
FIGURE 2.
WT CD45^{+} fibrocytes increased metastasis in *Ccr5*^{−/−} mice via *Mmp9*. (**A**) Bar graphs depicting the number of metastases in WT and *Ccr5*^{−/−} (R5) mice following the injection of 1×10^5 WT or *Ccr5*^{−/−} fibrocytes (Fcyte); 7.5×10^5 B16-F10 melanoma cells were injected i.v. 24 h after fibrocytes. Metastases were counted 2 wk later (*n* = 50). (**B**) Bar graphs depicting metastasis in *Ccr5*^{−/−} mice (*left*) and *Ccr5*^{−/−} mice following injection with either 1×10^5 WT fibroblasts (Fblasts) or fibrocytes (Fcytes; *n* = 26). (**C**) Bar graphs showing metastasis in *Ccr5*^{−/−} and Mmp9^{−/−} (M9) mice following injection with WT or *Mmp9*^{−/−} fibrocytes (*n* = 92). (**D**) Bar graph showing metastasis in mice without fibrocyte injection. WT mice (solid black) had significantly more metastases than *Ccr5*^{−/−}, *Mmp9*^{−/−} or the double knockout *Mmp9*^{−/−} × *Ccr5*^{−/−} (checkerboard; *n* = 47).
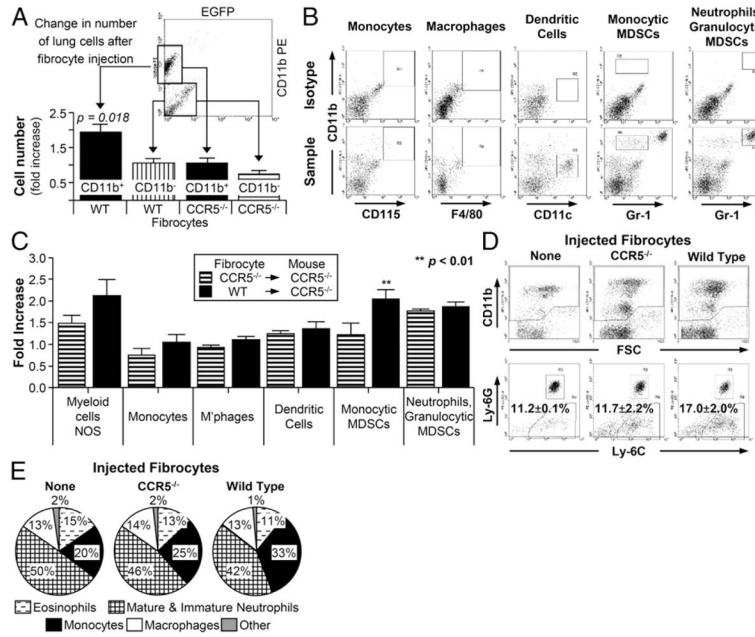
FIGURE 3.
WT fibrocytes recruited Ly-6$^+$, Ly-6G^{lo} cells in *Ccr5*$^{-/-}$ mice. (**A**) CD11b$^+$ cells were increased in *Ccr5*$^{-/-}$ mice 24 h after the injection of WT EGFP$^+$ fibrocytes. Dot plot shows gating strategy for calculating CD11b$^+$ cell number. The bar graph shows the fold increases of CD11b$^+$ (black bars) and CD11b$^-$ (striped; $n = 22$). (**B**) Gating strategy for the identification of CD11b$^+$ cells after injection with WT fibrocytes. The top row of dot plots were stained with isotype controls; the bottom row plots were stained with CD115, F4/80, CD11c, and Gr-1. (**C**) Bar graphs depicting fold induction of cell subpopulations following injection with *Ccr5*$^{-/-}$ (striped) or WT (solid) fibrocytes. Significant fold induction was seen in only monocytic MDSCs ($n = 20$). (**D**) Dot plots from *Ccr5*$^{-/-}$ mice following the injection of *Ccr5*$^{-/-}$ (*center*) or WT (*right*) fibrocytes. Ly-6C$^+$, Ly-6G$^-$ were significantly increased after injection of WT cells. (**E**) Differential percentages of CD11b$^+$ cells as detected on cytospin preparations. All differentials performed on CD11b$^+$ cells from *Ccr5*$^{-/-}$ mice after injection with WT fibrocytes (*left*), *Ccr5*$^{-/-}$ fibrocytes (*center*) or no fibrocytes (*right; $n = 24$).
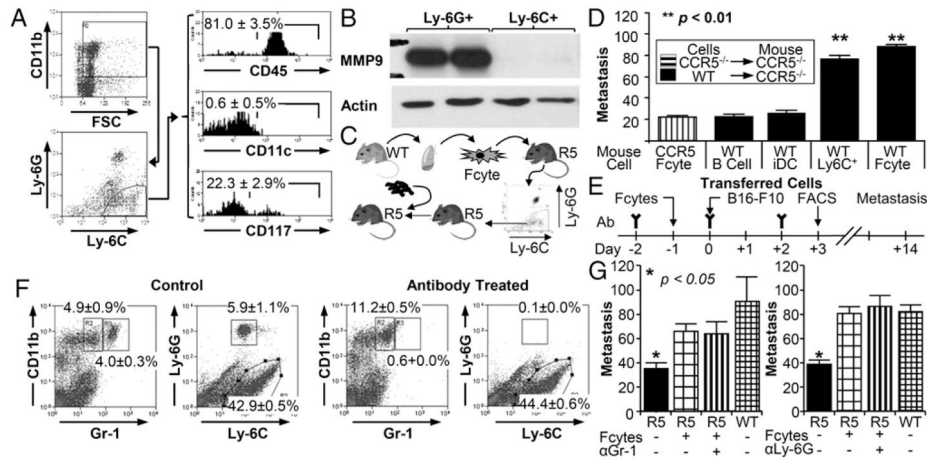
FIGURE 4.
Ly-6C[+], Ly-6G^{lo} cells recruited by fibrocytes promoted metastasis. (**A**) Flow cytometric analysis of Ly-6G^{lo}, Ly-6C^{+} cells. Gating strategy is on the *left*; histograms for CD45, CD11c, and CD117 are given on the *right* ($n = 5$). (**B**) Western blot analysis of Ly-6G^{lo}, Ly-6C^{+} cells isolated from Ccr5^{−/−} mice by flow sorting following injection with WT fibrocytes. (**C**) Experimental schema for defining function of Ly-6C^{+} monocytes. Ly-6C^{+} cells were isolated from *Ccr5*[−/−](R5) mice 24 h after fibrocyte injection and transferred into R5 mice. Tumor cells were injected within 4 h of monocyte injection. (**D**) Bar graph shows metastasis in *Ccr5*^{−/−} mice injected with *Ccr5*^{−/−} fibrocytes or 5×10^6 WT B cells, 1×10^6 WT immature dendritic cells (iDCs), 2×10^5 WT Ly-6C^{+} monocytes, or WT fibrocytes ($n = 42$). (**E**) Experimental schema for the depletion Gr-1 cells. Gr-1 or Ly-6G Ab was given on days −2,, 0, and 2 in relationship to the i.v. injection of B16 F10 cells (day zero). Fibrocytes (1×10^5) were given on day −1; flow cytometry was performed on day 3. (**F**) Representative dot plots of pulmonary cells from mice treated with either Gr-1 or Ly-6G Ab. The graph on the left includes all cells (excluding debris by FSC/SSC); the graph on the *right* represents only CD11b^{+} cells. (**G**) Bar graph displaying the number of metastasis in mice treated with Gr-1 ($n = 15$) or Ly-6G ($n = 31$) Ab. Untreated *Ccr5*^{−/−} mice (black) had statistically fewer metastases than all other groups. There were no significant differences in *Ccr5*^{−/−} mice injected with WT fibrocytes.
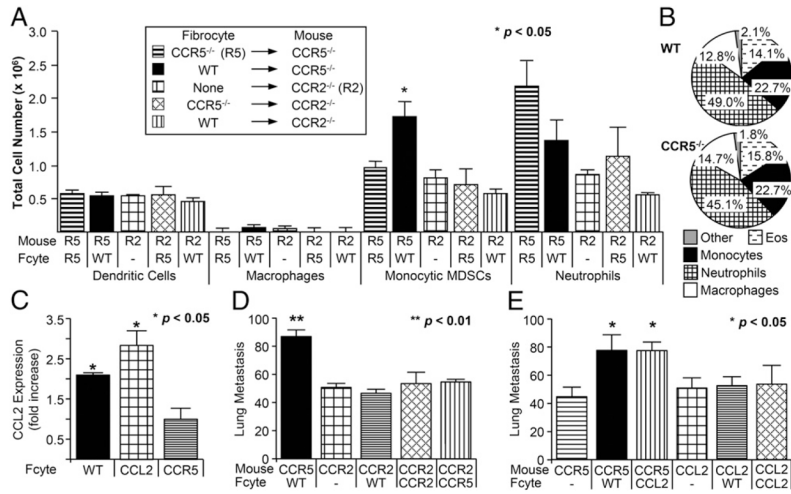
FIGURE 5.
Fibrocytes recruited premetastatic monocytes via CCR2. (**A**) Bar graphs depicting total number of cells for each subpopulation following the injection with $Ccr5^{-/-}$ (R5), $Ccr2^{-/-}$ (R2), or WT fibrocytes. Significant increase was seen in monocytic MDSCs only. (**B**) Pie graphs showing differential percentages of CD11b$^+$ cells as detected on cytospin preparations. All differentials performed on CD11b$^+$ cells from $Ccr2^{-/-}$ mice after injection with WT (*top*) or Ccr5$^{-/-}$ fibrocytes (*bottom*). (**C**) Bar graph depicting fold increase in $Ccl2$ mRNA expression in $Ccr5^{-/-}$ mice following injection with WT, $Ccl2^{-/-}$, or $Ccr5^{-/-}$ fibrocytes ($n = 16$). (**D**) Bar graph representing lung metastasis in $Ccr5^{-/-}$ or $Ccr2^{-/-}$ mice injected with WT, $Ccr2^{-/-}$, or $Ccr5^{-/-}$ fibrocytes ($n = 72$). (**E**) Bar graph showing the number of metastases in $Ccr5^{-/-}$ or $Ccl2^{-/-}$ after the injection of WT or $Ccl2^{-/-}$ fibrocytes (Fcyte; $n = 70$).